

Use of SVM Methods with Surface-Based Cortical and Volumetric Subcortical Measurements to Detect Alzheimer's Disease

Pedro Paulo de Magalhães Oliveira Jr.^{a,*}, Ricardo Nitri^b, Geraldo Busatto^c, Carlos Buchpiguel^d, João Ricardo Sato^a and Edson Amaro Jr.^a

^a*NIF – Neuroimagem Funcional, Departamento de Radiologia da Faculdade de Medicina do Hospital das Clínicas da Faculdade de Medicina da Universidade de São Paulo, Brazil*

^b*Departamento de Neurologia da Faculdade de Medicina do Hospital das Clínicas da Faculdade de Medicina da Universidade de São Paulo, Brazil*

^c*LIM21 – Instituto de Psiquiatria da Faculdade de Medicina do Hospital das Clínicas da Faculdade de Medicina da Universidade de São Paulo, Brazil*

^d*Medicina Nuclear, Departamento de Radiologia da Faculdade de Medicina do Hospital das Clínicas da Faculdade de Medicina da Universidade de São Paulo, Brazil*

Accepted 27 October 2009

Abstract. Here, we examine morphological changes in cortical thickness of patients with Alzheimer's disease (AD) using image analysis algorithms for brain structure segmentation and study automatic classification of AD patients using cortical and volumetric data. Cortical thickness of AD patients ($n = 14$) was measured using MRI cortical surface-based analysis and compared with healthy subjects ($n = 20$). Data was analyzed using an automated algorithm for tissue segmentation and classification. A Support Vector Machine (SVM) was applied over the volumetric measurements of subcortical and cortical structures to separate AD patients from controls. The group analysis showed cortical thickness reduction in the superior temporal lobe, parahippocampal gyrus, and entorhinal cortex in both hemispheres. We also found cortical thinning in the isthmus of cingulate gyrus and middle temporal gyrus at the right hemisphere, as well as a reduction of the cortical mantle in areas previously shown to be associated with AD. We also confirmed that automatic classification algorithms (SVM) could be helpful to distinguish AD patients from healthy controls. Moreover, the same areas implicated in the pathogenesis of AD were the main parameters driving the classification algorithm. While the patient sample used in this study was relatively small, we expect that using a database of regional volumes derived from MRI scans of a large number of subjects will increase the SVM power of AD patient identification.

Keywords: Alzheimer's disease, FreeSurfer, magnetic resonance imaging, support vector machine, surface based methods

INTRODUCTION

Alzheimer's disease (AD) is the most prevalent cause of dementia in elderly people [1]. In the last two

decades, the comprehension of the underlying mechanisms of elderly dementia and AD have been enlightened by evidence emerging from different research fields, perhaps with more contribution arising from neuropathology, genetics [2], and neuroimaging [3] data.

Current literature from neuropathology and neuroimaging studies shows evidence that common changes can be found in AD patients, but unfortunately, these are neither specific nor diagnostic at an individual level. The most celebrated anatomical finding is a volumetric

*Correspondence to: Pedro Paulo de Magalhães Oliveira Jr., Rua Dr. Enéas de Carvalho Aguiar, s/n, InRad – Instituto de Radiologia – Setor de RM, São Paulo – SP, CEP 05403-900, Brazil. Tel.: +55 11 3069 7919; E-mail: ppj@netfilter.com.br.

reduction in the hippocampal formation and parahippocampal gyrus [4,5]. However, in earlier stages of the disease, there is no evidence that this finding can be used as a diagnostic criterion. Rather, volumetric assessment of the hippocampal formation seems to be more specific at an individual level when analyzing temporal progression [6]. Imaging data can provide insights of how the disease progresses in time at each brain structure from a macroscopic viewpoint.

The high variability of AD phenotypes, a broad range of clinical presentations, and the role of cognitive reserve in disease progression are confounding factors in creating a generic neuroimaging criterion for AD diagnosis. A promising approach is to study groups of AD patients showing common patterns (old age, mild cognitive impairment, high education, apolipoprotein E (ApoE) ϵ 4 carriers, etc.) in order to assess the power of specific techniques in differentiating patients from healthy volunteers – then proceed with further steps to design diagnostic tests that can be applied in all types of AD patients.

Some studies have explored artificial intelligence and machine learning methods to detect cerebral changes and discriminate normal aging from AD [7–11]. This marker (obtained from MRI data alone) is neither fully conclusive nor predictive of the outcome, in spite of the frequently reported correlation between cerebral atrophy and symptoms. Nevertheless, some studies showed that machine learning methods are a reliable tool for indicating the presence of probable AD, even compared to conventional radiological analysis [12].

However, new methods for early detection and early estimation of treatment outcome are needed [13] as specific treatment drugs for dementia aimed to delay the progression of disease (in terms of brain degeneration effects) [1,14] are emerging on a daily basis. Perhaps the combination between surrogate markers (laboratory, genetic, and quantitative neuroimaging data) with automated classification algorithms may play an important role in detecting subtle changes preceding AD clinical manifestations.

Support vector machines (SVM) are a broad term to refer to a group of supervised learning methods that tries to maximize the distance of a hyperplane or hypersurface separating two classes [15]. Machine learning techniques have been applied in several science fields, including neuroscience [16,17]. SVM allows classification of both linear and non-linear separable data. It has been used to detect AD using mostly voxel-based morphometry (VBM) and sometimes VBM with auxiliary data (ApoE ϵ 4 mutation, PET) [8,10]. One study

used SVM in conjunction with surface based analysis to separate AD patients from healthy controls [11], and another recent study used the same technique to classify AD using cortical parcellation data [18].

In this study, our aim is to: 1) use surface based morphometry techniques to study cortical thickness differences between healthy controls and AD patients; 2) use SVM classifiers based on parameters extracted from MR images to separate patients with AD from healthy controls; and 3) compare this multivariate method with a single variable classifier.

MATERIAL AND METHODS

Study groups

Fourteen patients with AD from an outpatient unit in the city of São Paulo, Brazil (Department of Psychiatry, University of São Paulo) were interviewed with the Cambridge Mental Disorders of the Elderly Examination (CAMDEX) [19]. All met NINDS/ADRDA criteria for probable AD [20]. They also passed screening laboratory examinations including complete blood count; liver, renal, and thyroid function tests; and Vitamin B12 and folate levels. The exclusion criteria included positive syphilis serology, a Hachinski Ischemic score ≥ 4 , Parkinson's disease, non-neuroleptic induced Parkinson-like syndrome, hyperthyroidism, hyperparathyroidism, diabetes mellitus, other psychiatric disorders (schizophrenia, obsessive compulsive disorder), claustrophobia, chronic use of neuroleptics, and previous use of cholinesterase inhibitor. The same exclusion criteria were used to select a control group of normal elderly subjects ($n = 20$). They were free of symptoms suggestive of physical or mental disorder based on the CAMDEX interview, general medical questioning, and physical and neurological examination.

The overall severity of cognitive impairment was rated with the Mini-Mental State Examination (MMSE) [21]. The average MMSE in patients was 21.5 ± 2.27 and in the control group average MMSE was 27.9 ± 1.44 . The average onset time of the symptoms in AD group was 22.5 ± 11.4 months. Further details are shown in Table 1.

MRI acquisition

Images were acquired using a 1.5T GE Horizon LX 8.3 scanner (General Electric Medical Systems, Mil-

Table 1
Clinical, demographic and neuropsychological characteristics of AD subjects ($n = 14$) and healthy controls ($n = 20$). Age ($p = 0.027$)

Code	Gender	Age	Diagnosis	Education (years)	Family history for AD	MMSE	Symptom onset (months)
ALZ01	M	78	AD	17	N	24	28
ALZ02	F	77	AD	12	N	26	12
ALZ03	F	70	AD	4	N	19	24
ALZ04	M	68	AD	9	S	21	36
ALZ05	F	80	AD	4	N	20	12
ALZ06	M	74	AD	10	N	21	36
ALZ07	M	77	AD	4	N	22	24
ALZ08	F	76	AD	4	N	22	18
ALZ09	F	76	AD	8	N	21	18
ALZ10	F	74	AD	4	S	18	24
ALZ11	M	84	AD	7	N	24	8
ALZ12	F	79	AD	12	S	24	18
ALZ13	M	79	AD	9	N	21	10
ALZ14	M	75	AD	4	S	19	48
CTL01	F	80	CTL	8	N	28	N/A
CTL02	F	74	CTL	4	N	28	N/A
CTL03	F	75	CTL	15	N	27	N/A
CTL04	M	76	CTL	11	N	28	N/A
CTL05	M	76	CTL	4	N	26	N/A
CTL06	F	72	CTL	16	N	29	N/A
CTL07	F	70	CTL	5	N	26	N/A
CTL08	M	80	CTL	4	N	26	N/A
CTL09	F	68	CTL	8	N	29	N/A
CTL10	M	71	CTL	16	N	29	N/A
CTL11	M	75	CTL	8	N	27	N/A
CTL12	M	75	CTL	4	N	25	N/A
CTL13	M	68	CTL	11	N	30	N/A
CTL14	M	73	CTL	11	N	29	N/A
CTL15	M	75	CTL	4	N	27	N/A
CTL16	F	74	CTL	16	N	29	N/A
CTL17	F	75	CTL	15	N	29	N/A
CTL18	F	66	CTL	16	N	30	N/A
CTL19	F	66	CTL	15	N	29	N/A
CTL20	F	70	CTL	4	N	27	N/A

M – male F – female; AD – Alzheimer’s disease, CTL – Control; N – Not present; Y – Present; N/A – Not applicable.

waukee). A series of contiguous 1.6 mm thick coronal images across the entire brain were acquired, using a T1-weighted fast field echo sequence (TE = 9 ms, TR = 27 ms, flip angle = 30°, field of view = 240 mm, 256 × 256 matrix), acquired perpendicular to the main temporal axis.

Image analysis

Cortical reconstruction and volumetric segmentation was performed with the FreeSurfer image analysis suite (version 4.3.0), which is documented and freely available for download online (<http://surfer.nmr.mgh.harvard.edu/>). The technical details of these procedures are described in previous publications [22–28]. Briefly, this processing includes removal of non-brain tissue using a hybrid watershed/surface deformation procedure [29], automated Talairach transformation, segmentation of the subcortical white matter and deep gray

matter volumetric structures (including hippocampus, amygdala, caudate, putamen, ventricles) [26,27], intensity normalization [30], tessellation of the gray matter white matter boundary, automated topology correction [28,31], and surface deformation following intensity gradients to optimally place the gray/white and gray/cerebrospinal fluid (CSF) borders at the location where the greatest shift in intensity defines the transition to the other tissue class [22,23].

Once the cortical models are complete, a number of deformable procedures can be performed for further data processing and analysis including surface inflation [24]; registration to a spherical atlas which utilized individual cortical folding patterns to match cortical geometry across subjects [32]; parcellation of the cerebral cortex into units based on gyral and sulcal structure [25,33]; and creation of a variety of surface based data including maps of curvature and sulcal depth.

This method uses both intensity and continuity information from the entire three dimensional MR volume in segmentation and deformation procedures to produce representations of cortical thickness, calculated as the closest distance from the gray/white boundary to the gray/CSF boundary at each vertex on the tessellated surface [22]. The maps are created using spatial intensity gradients across tissue classes and are therefore not simply reliant on absolute signal intensity. The maps produced are not restricted to the voxel resolution of the original data thus are capable of detecting submillimeter differences between groups. Procedures for the measurement of cortical thickness have been validated against histological analysis [34] and manual measurements [35,36]. FreeSurfer morphometric procedures have been demonstrated to show good test-retest reliability across scanner manufacturers and across field strengths [37].

Statistical analysis

Step 1: The group analysis of cortical thickness was performed using **mri_glmfit** from FreeSurfer, using a general linear model over a common spherical coordinate system [32] to produce a surface map of cortical thickness difference comparing controls and AD patients. We do not use this step for classification but to visualize where the cortex of AD patients is thinner than controls.

Step 2: The volume measurement of cortical and subcortical structures obtained from FreeSurfer was used to train a multivariate classifier: a support vector machine (SVM) using a radial basis function (RBF) kernel [$k(x, x') = \exp(\gamma|x-x'|^2)$].

Cost and γ , for the RBF were estimated using the grid-search algorithm: pairs of (Cost, γ) are tried and the one producing the best cross-validation accuracy is chosen [38].

Step 3: The training step was used to detect and remove the volume structures not relevant to discriminate patients with AD from controls. This feature selection, over volumetric measures, was performed in a software developed by one of the authors [PPM] using LibSVM [38]. The software executes the following procedure:

1. To train SVM using all features: (Volume of 45 areas, each volume is a feature)
2. Compute cross validation leave-one-out accuracy for step 1.
3. From the 45 areas, eliminate the features whose F-Score is lower than 10% of the largest F-Score.

4. For each of all combination of the remaining areas execute:
 - a. To train the SVM using only the subset of the combination's features
 - b. Compute cross validation leave-one-out for step 3a
 - c. Save the feature subset if the value of 3b is equal the value of step 2 and the number of features is smaller than previously obtained.

Step 4: A ROC curve for the volume of each individual brain structure was constructed to verify whether a multivariate classifier was needed.

RESULTS

The group analysis of cortical thickness among patients with AD and the healthy aged-matched control group showed areas of cortical reduction ($p < 0.01$, corrected for multiple comparisons with false discovery rate) in the superior temporal lobe, parahippocampal gyrus, and entorhinal cortex in both hemispheres. In the right hemisphere, we also found the reduction in isthmus of cingulate gyrus and middle temporal gyrus. In both hemispheres, there is a small area of cortical thinning in AD patients in superior frontal lobe (Fig. 1).

The volume from the 45 brain areas calculated with FreeSurfer automatic segmentation and volume estimation (Table 2) has been used as an input to train a SVM with RBF kernel ($\gamma = 0.0078125$ and Cost=8.0). This technique produced a discriminating power of 88.2% [CI_{95%}; 72.5%–96.7%] (Sensitivity=92.8% [CI_{95%}; 66.1%–99.8%], Specificity=85.0% [CI_{95%}; 62.1%–96.8%]) using cross validation with leave-one-out.

When analyzing the classification provided by each of the 45 areas alone, left and right hippocampi, as well as overall cortical thickness were the most relevant features, to classification using ROC areas. Nevertheless, SVM outperforms the classification produced from each feature alone (Fig. 2).

The feature selection in the SVM revealed areas relevant to discriminate AD patients and normal controls comprising anterior and posterior corpus callosum volume, left and right hippocampus, right lateral ventricular horn size, and right gray matter volume (Table 3).

The scatter plot matrix showing from this multidimensional data shows a variable power for each parameter contributing to the classification, as well as individual patients and groups produced (Fig. 3).

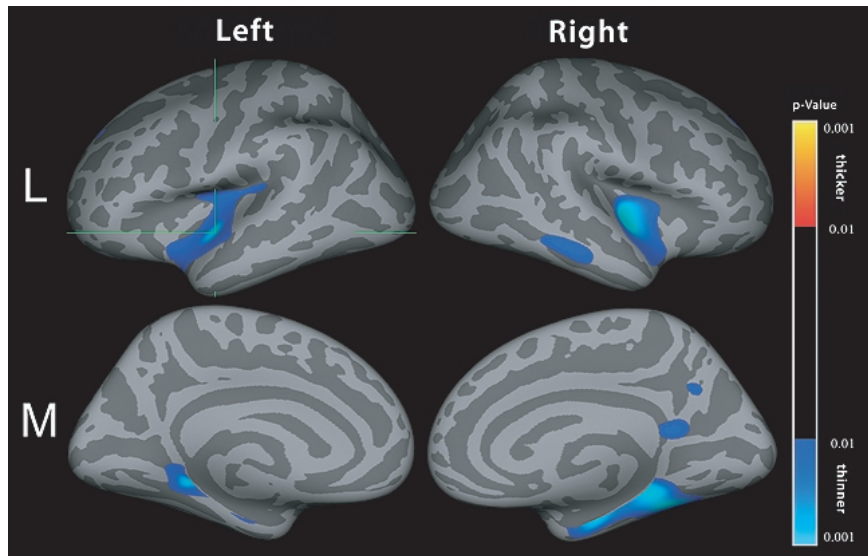


Fig. 1. Comparison of cortical thickness of patients with AD versus healthy elderly controls using age as a covariate. Left and right hemisphere of group analysis showing thinning in AD patients are displayed in Lateral (L) and Medial (M) views. Colors are mapped to p-values using the color scale attached.

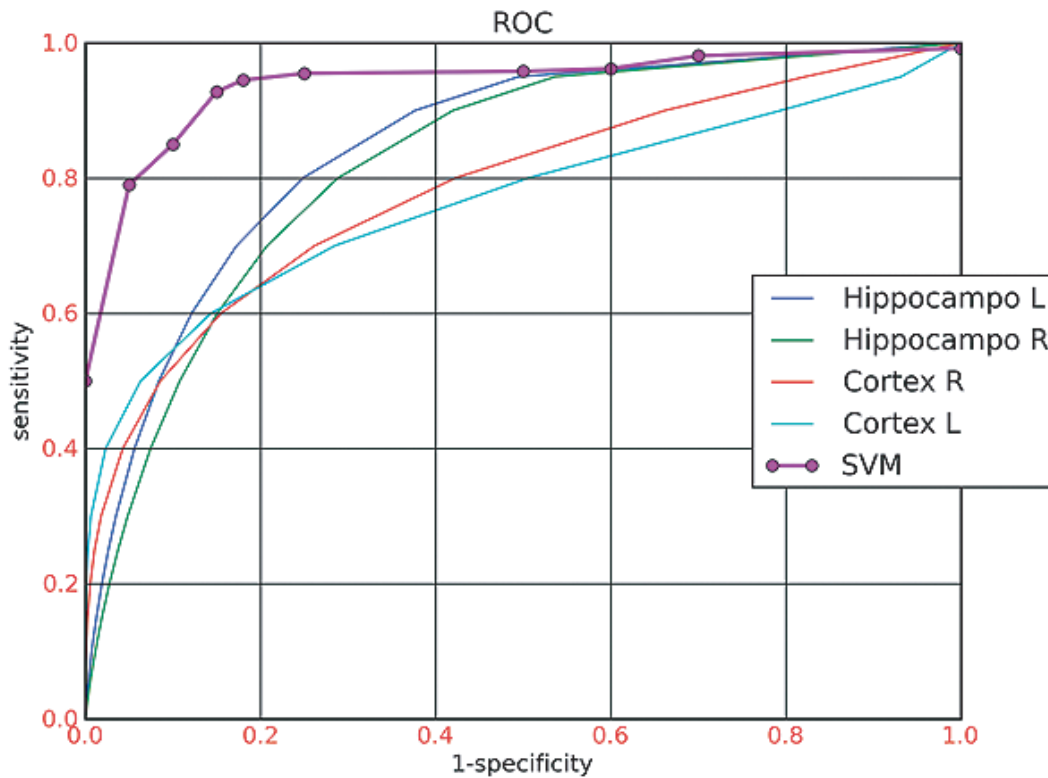


Fig. 2. ROC (receiver operating characteristic). Curve of the variables used in SVM classification showing that the multivariate classifier used has more accurate results than using any of the variables alone. SVM ROC has been created with distinct trainings using distinct weights in the cost function.

Table 2
Volumetric Structures used in the SVM classification model

Right Cerebellum White Matter	Right Ventral Diencephalon
Right choroid plexus	Left Putamen
Left Amygdala	Left Cerebral White Matter
Left Cerebellum White Matter	Corpus Callosum Medial Anterior
Right Thalamus Proper	Right Putamen
Right Pallidum	Left Accumbens area
Left Ventral Diencephalon	Right Amygdala
Right Accumbens area	Left Thalamus Proper
Right Cerebral White Matter	Left Cerebellum Cortex
Corpus Callosum Medial Posterior	Left Lateral Ventricle
Right Lateral Ventricular Horn	Right Cerebellum Cortex
Corpus Callosum Central	Left vessel
Brain Stem	Left choroid plexus
Right Hippocampus	Left Caudate
Right Caudate	Left Lateral Ventricular Horn
Corpus Callosum Posterior	Left Cerebral Cortex
Corpus Callosum Anterior	Right Cerebral Cortex
Right Lateral Ventricle	Right vessel
Left Hippocampus	Optic Chiasm
Left Pallidum	4th Ventricle
3rd Ventricle	5th Ventricle

Table 3
Volumetric Structures useful to SVM prediction, ordered by importance in SVM model

Anatomic region	Volume patients (mm ³)	Volume control (mm ³)
Right Lateral Ventricular Horn	1360 mm ³ ± 989	570 mm ³ ± 267
Left Hippocampus	2581 mm ³ ± 499	3271 mm ³ ± 452
Right Hippocampus	2862 mm ³ ± 615	3596 mm ³ ± 508
Left Cerebral Cortex	194093 mm ³ ± 14 × 10 ³	212592 mm ³ ± 19 × 10 ³
Right Cerebral Cortex	193095 mm ³ ± 12 × 10 ³	212620 mm ³ ± 19 × 10 ³
Corpus Callosum Posterior	1771 mm ³ ± 72.03	877 mm ³ ± 100
Corpus Callosum Anterior	596 mm ³ ± 87.42	751 mm ³ ± 122

DISCUSSION

We show that a group of patients with AD compared to a matched population have a reduction in cortical thickness when analyzing MRI data using a surface based method. The cortical surface analysis findings in our AD sample replicate previous reports in the neuroimaging literature [4,39–41]. The cortical thinning in temporal, limbic, and entorhinal cortex confirms the previous literature on cortical thickness analysis and surface based volumetric analysis of AD [40,41]. In addition, the findings in AD with mild to moderate impairment or recent onset [4,39] regarding cortical volume decrease occurring centered on medial temporal lobes, are confirmed in this study. However, our results have some differences from previous reports: parietal cortex did not show significant thinning in AD compared to controls, and the right brain hemisphere showed more alteration both in surface based and volumetric measurement techniques. We have also shown that the SVM analysis showed a good performance to classify

AD patients and healthy controls as well in identifying anatomic structures that have a reduced volume in AD patients.

In imaging studies of AD, it is usual to find differences either metabolic or volumetric in parietal cortex [5]. We did not find evidence of a parietal cortex involvement, maybe due to the lack of statistical power. However, this finding is consistent with the hypothesis that in this particular group of older patients with recent onset, there is less involvement of the parietal lobe. Other studies with groups with mild to moderate impairment [39] showed that the predominant differences are in the temporal lobe. A hypothesis is that these patients may have developed AD symptoms later in life simply because of particular disease mechanisms, which *per se* could induce to a more delayed progression with less cortex involvement.

The findings presented here reinforce the importance of image studies of AD in all subgroups. Previous reports have concentrated on findings from mild impairment [3,39], but these actually may reflect changes

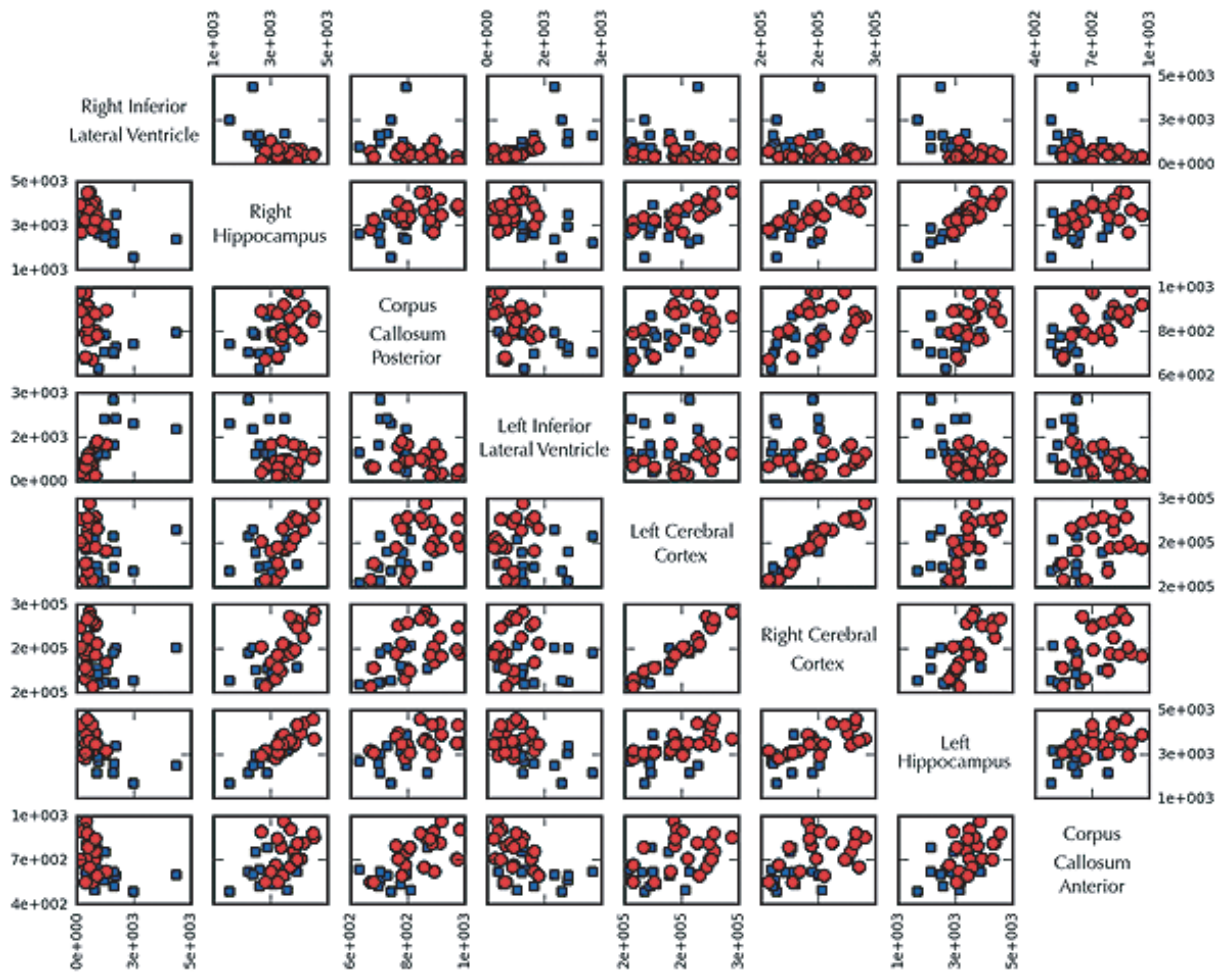


Fig. 3. Scatter plot matrix of the eight volumetric features used in SVM classification. This figure helps visualizing the multidimensional data used to classify between AD patients and healthy controls. Blue squares represent AD patients and red dots represent healthy controls. The volumes of brain structures are given in mm^3 .

specific to a subgroup of patients, and therefore the alterations at this initial phase can be difficult to detect if one only looks for a predetermined pattern. Patients with recent symptoms, late or early onset, high or low education level, or positive ApoE4 mutation [41,42] may provide distinct features to be pursued in order to discriminate mechanisms of AD damage in nervous system.

The differences between cortical thinning from right to left hemispheres are not easy to explain. One possible theory for these findings is that degeneration is distinct in the dominant hemisphere [43]. Another possible explanation is the progressive degeneration pattern affecting language in a later stage, after the usual initial compromise found in olfaction and memory. However, this finding requires further study to determine whether

it is a constant feature of AD or an artifact produced by the methodology used, data outliers, or a small sample. Further studies are required to analyze this effect properly.

We have also introduced the use of SVM as a trained classifier to detect AD based only in the volume of subcortical structures and cerebral cortex with data obtained using a surface based approach. Similar techniques have been also studied with voxel based morphometry (VBM) [9,44], combining VBM with ApoE ϵ 4 marker [10], with cortical thickness [11], using VBM with a cortical parcellation atlas [18], and combining VBM with PET data [45]. Most of the results presented here confirm the previous published papers regarding classification of AD patients using machine learning techniques [9–11,44]. Also the classification

accuracy in this present study is similar with the above mentioned publications, considering the sample size used. However, we noticed very interesting converging results emerging from a completely different image analysis approach, free from the formalisms of classic statistical assumptions, and with the power of providing patterns emerging from data behavior, without a priori constraints. We believe that our results help to add information related to the robustness of findings in specific cortical regions. If this marker is reproducible at an individual level, it represents another tool that is able to provide parameters to guide neurologists' decisions about when to start any available medical treatment.

One possible issue regarding the SVM results presented in this paper is whether they are novel results or lack originality compared to previously published studies. We believe the differences of our work to the cited papers are, among others:

1. Use of a surface based method software in order to generate automatically the measures.
2. Use of subcortical structures volumes as a classifier feature.
3. Study cortical thickness difference between the two groups to ensure that the data is comparable with other cortical thickness studies.

The paper from Lerch and colleagues [11] indeed uses surface based methods, however, it relies on cortical thickness only as an input feature to the classifier while we used the volume of gray matter, white matter, and subcortical structures to train the SVM.

The results shown here were obtained with a very recent version of FreeSurfer, optimized to estimate the volumes of cortical and sub-cortical structures. This software is a freeware, has a sound reliability, and has been used in many published articles [37]. We believe the SVM approach shown here can be used to compare classification performance in different populations and subtypes of the disease in multicentre studies.

Another point worth mentioning is that our findings are in the same line as results from recent neuropathological studies [46], pointing out that a diagnosis of AD is virtually impossible on a routine basis – thus making the search for a biomarker for AD very challenging. At the same time, clinical evaluation is a subjective estimate and prone to errors, not to mention that there is no clear-cut estimate of patient prognosis from a structured diagnostic criterion. SVM and other specialized statistical classification methods based on image are promising techniques to improve the diagnosis and monitor the progression of AD.

ACKNOWLEDGMENTS

The authors would like to thank B. Fischl, L. Zollei, A. Stevens, and N. Schmansky for helpful comments and support on the FreeSurfer functioning. The authors also thank the anonymous reviewers for their comments that helped much in the paper final version.

Authors' disclosures available online (<http://www.j-alz.com/disclosures/view.php?id=191>).

REFERENCES

- [1] Pangalos MN, Schechter LE, Hurko O (2007) Drug development for CNS disorders: strategies for balancing risk and reducing attrition. *Nat Rev Drug Discov* **6**, 521-532.
- [2] McCarron MO, Nicoll JA, Stewart J, Ironside JW, Mann DM, Love S, Graham DI, Dewar D (1999) The apolipoprotein E epsilon2 allele and the pathological features in cerebral amyloid angiopathy-related hemorrhage. *J Neuropathol Exp Neurol* **58**, 711-718.
- [3] Dickerson BC, Bakkour A, Salat DH, Feczko E, Pacheco J, Greve DN, Grodstein F, Wright CI, Blacker D, Rosas HD, Sperling RA, Atri A, Growdon JH, Hyman BT, Morris JC, Fischl B, Buckner RL (2009) The cortical signature of Alzheimer's disease: regionally specific cortical thinning relates to symptom severity in very mild to mild ad dementia and is detectable in asymptomatic amyloid-positive individuals. *Cereb Cortex* **19**, 497-510.
- [4] Fox NC, Warrington EK, Freeborough PA, Hartikainen P, Kennedy AM, Stevens JM, Rossor MN (1996) Presymptomatic hippocampal atrophy in Alzheimer's disease. A longitudinal MRI study. *Brain* **119** (Pt 6), 2001-2007.
- [5] Foundas AL, Leonard CM, Mahoney SM, Agee OF, Heilman KM (1997) Atrophy of the hippocampus, parietal cortex, and insula in Alzheimer's disease: a volumetric magnetic resonance imaging study. *Neuropsychiatry Neuropsychol Behav Neurol* **10**, 81-89.
- [6] Colliot O, Chetelat G, Chupin M, Desgranges B, Magnin B, Benali H, Dubois B, Garnero L, Eustache F, Lehericy S (2008) Discrimination between Alzheimer disease, mild cognitive impairment, and normal aging by using automated segmentation of the hippocampus. *Radiology* **248**, 194-201.
- [7] Thompson PM, Hayashi KM, Dutton RA, Chiang MC, Leow AD, Sowell ER, De Zubicaray G, Becker JT, Lopez OL, Aizenstein HJ, Toga AW (2007) Tracking Alzheimer's disease. *Ann N Y Acad Sci* **1097**, 183-214.
- [8] Fan Y, Batmanghelich N, Clark CM, Davatzikos C (2008) Spatial patterns of brain atrophy in MCI patients, identified via high-dimensional pattern classification, predict subsequent cognitive decline. *Neuroimage* **39**, 1731-1743.
- [9] Kloppel S, Stonnington CM, Chu C, Draganski B, Scahill RI, Rohrer JD, Fox NC, Jack CR, Jr., Ashburner J, Frackowiak RS (2008) Automatic classification of MR scans in Alzheimer's disease. *Brain* **131**, 681-689.
- [10] Vemuri P, Gunter JL, Senjem ML, Whitwell JL, Kantarci K, Knopman DS, Boeve BF, Petersen RC, Jack CR, Jr. (2008) Alzheimer's disease diagnosis in individual subjects using structural MR images: validation studies. *Neuroimage* **39**, 1186-1197.

- [11] Lerch JP, Pruessner J, Zijdenbos AP, Collins DL, Teipel SJ, Hampel H, Evans AC (2008) Automated cortical thickness measurements from MRI can accurately separate Alzheimer's patients from normal elderly controls. *Neurobiol Aging* **29**, 23-30.
- [12] Kloppel S, Stonnington CM, Barnes J, Chen F, Chu C, Good CD, Mader I, Mitchell LA, Patel AC, Roberts CC, Fox NC, Jack CR, Jr., Ashburner J, Frackowiak RS (2008) Accuracy of dementia diagnosis: a direct comparison between radiologists and a computerized method. *Brain* **131**, 2969-2974.
- [13] Tanaka Y, Hanyu H, Sakurai H, Shimizu S, Takasaki M (2003) [Characteristics of MRI features in Alzheimer's disease patients predicting response to donepezil treatment]. *Nippon Ronen Igakkai Zasshi* **40**, 261-266.
- [14] Ames D, Kaduszkiewicz H, van den Bussche H, Zimmermann T, Birks J, Ashby D (2008) For debate: is the evidence for the efficacy of cholinesterase inhibitors in the symptomatic treatment of Alzheimer's disease convincing or not? *Int Psychogeriatr* **20**, 259-292.
- [15] Boser BE, Guyon IM, Vapnik VN (1992) in *Proceedings of the fifth annual workshop on Computational learning theory* (ACM, Pittsburgh, Pennsylvania, United States).
- [16] Fu CH, Mourao-Miranda J, Costafreda SG, Khanna A, Marquand AF, Williams SC, Brammer MJ (2008) Pattern classification of sad facial processing: toward the development of neurobiological markers in depression. *Biol Psychiatry* **63**, 656-662.
- [17] Marquand AF, Mourao-Miranda J, Brammer MJ, Cleare AJ, Fu CH (2008) Neuroanatomy of verbal working memory as a diagnostic biomarker for depression. *Neuroreport* **19**, 1507-1511.
- [18] Magnin B, Mesrob L, Kinkingnehun S, Pelegrini-Issac M, Colliot O, Sarazin M, Dubois B, Lehericy S, Benali H (2009) Support vector machine-based classification of Alzheimer's disease from whole-brain anatomical MRI. *Neuroradiology* **51**, 73-83.
- [19] Roth M, Tym E, Mountjoy CQ, Huppert FA, Hendrie H, Verma S, Goddard R (1986) CAMDEX. A standardised instrument for the diagnosis of mental disorder in the elderly with special reference to the early detection of dementia. *Br J Psychiatry* **149**, 698-709.
- [20] McKhann G, Drachman D, Folstein M, Katzman R, Price D, Stadlan EM (1984) Clinical diagnosis of Alzheimer's disease: report of the NINCDS-ADRDA Work Group under the auspices of Department of Health and Human Services Task Force on Alzheimer's Disease. *Neurology* **34**, 939-944.
- [21] Folstein MF, Folstein SE, McHugh PR (1975) "Mini-mental state". A practical method for grading the cognitive state of patients for the clinician. *J Psychiatr Res* **12**, 189-198.
- [22] Fischl B, Dale AM (2000) Measuring the thickness of the human cerebral cortex from magnetic resonance images. *Proc Natl Acad Sci USA* **97**, 11050-11055.
- [23] Dale AM, Fischl B, Sereno MI (1999) Cortical surface-based analysis. I. Segmentation and surface reconstruction. *Neuroimage* **9**, 179-194.
- [24] Fischl B, Sereno MI, Dale AM (1999) Cortical surface-based analysis. II: Inflation, flattening, and a surface-based coordinate system. *Neuroimage* **9**, 195-207.
- [25] Fischl B, van der Kouwe A, Destrieux C, Halgren E, Segonne F, Salat DH, Busa E, Seidman LJ, Goldstein J, Kennedy D, Caviness V, Makris N, Rosen B, Dale AM (2004) Automatically parcellating the human cerebral cortex. *Cereb Cortex* **14**, 11-22.
- [26] Fischl B, Salat DH, van der Kouwe AJ, Makris N, Segonne F, Quinn BT, Dale AM (2004) Sequence-independent segmentation of magnetic resonance images. *Neuroimage* **23 Suppl 1**, S69-84.
- [27] Fischl B, Salat DH, Busa E, Albert M, Dieterich M, Haselgrove C, van der Kouwe A, Killiany R, Kennedy D, Klaveness S, Montillo A, Makris N, Rosen B, Dale AM (2002) Whole brain segmentation: automated labeling of neuroanatomical structures in the human brain. *Neuron* **33**, 341-355.
- [28] Fischl B, Liu A, Dale AM (2001) Automated manifold surgery: constructing geometrically accurate and topologically correct models of the human cerebral cortex. *IEEE Trans Med Imaging* **20**, 70-80.
- [29] Segonne F, Dale AM, Busa E, Glessner M, Salat D, Hahn HK, Fischl B (2004) A hybrid approach to the skull stripping problem in MRI. *Neuroimage* **22**, 1060-1075.
- [30] Sled JG, Zijdenbos AP, Evans AC (1998) A nonparametric method for automatic correction of intensity nonuniformity in MRI data. *IEEE Trans Med Imaging* **17**, 87-97.
- [31] Segonne F, Pacheco J, Fischl B (2007) Geometrically accurate topology-correction of cortical surfaces using nonseparating loops. *IEEE Trans Med Imaging* **26**, 518-529.
- [32] Fischl B, Sereno MI, Tootell RB, Dale AM (1999) High-resolution intersubject averaging and a coordinate system for the cortical surface. *Hum Brain Mapp* **8**, 272-284.
- [33] Desikan RS, Segonne F, Fischl B, Quinn BT, Dickerson BC, Blacker D, Buckner RL, Dale AM, Maguire RP, Hyman BT, Albert MS, Killiany RJ (2006) An automated labeling system for subdividing the human cerebral cortex on MRI scans into gyral based regions of interest. *Neuroimage* **31**, 968-980.
- [34] Rosas HD, Liu AK, Hersch S, Glessner M, Ferrante RJ, Salat DH, van der Kouwe A, Jenkins BG, Dale AM, Fischl B (2002) Regional and progressive thinning of the cortical ribbon in Huntington's disease. *Neurology* **58**, 695-701.
- [35] Kuperberg GR, Broome MR, McGuire PK, David AS, Eddy M, Ozawa F, Goff D, West WC, Williams SC, van der Kouwe AJ, Salat DH, Dale AM, Fischl B (2003) Regionally localized thinning of the cerebral cortex in schizophrenia. *Arch Gen Psychiatry* **60**, 878-888.
- [36] Salat DH, Buckner RL, Snyder AZ, Greve DN, Desikan RS, Busa E, Morris JC, Dale AM, Fischl B (2004) Thinning of the cerebral cortex in aging. *Cereb Cortex* **14**, 721-730.
- [37] Han X, Jovicich J, Salat D, van der Kouwe A, Quinn B, Czanner S, Busa E, Pacheco J, Albert M, Killiany R, Maguire P, Rosas D, Makris N, Dale A, Dickerson B, Fischl B (2006) Reliability of MRI-derived measurements of human cerebral cortical thickness: the effects of field strength, scanner upgrade and manufacturer. *Neuroimage* **32**, 180-194.
- [38] Chih-Chung C, Chih-Jen L (2009) LIBSVM: a library for support vector machines, <http://www.csie.ntu.edu.tw/~cjlin/libsvm>, Accessed November 22, 2009.
- [39] Singh V, Chertkow H, Lerch JP, Evans AC, Dorr AE, Kabani NJ (2006) Spatial patterns of cortical thinning in mild cognitive impairment and Alzheimer's disease. *Brain* **129**, 2885-2893.
- [40] Du AT, Schuff N, Kramer JH, Rosen HJ, Gorno-Tempini ML, Rankin K, Miller BL, Weiner MW (2007) Different regional patterns of cortical thinning in Alzheimer's disease and frontotemporal dementia. *Brain* **130**, 1159-1166.
- [41] Desikan RS, Fischl B, Cabral HJ, Kemper TL, Guttman CR, Blacker D, Hyman BT, Albert MS, Killiany RJ (2008) MRI measures of temporoparietal regions show differential rates of atrophy during prodromal AD. *Neurology* **71**, 819-825.
- [42] Jack CR, Jr., Shiung MM, Gunter JL, O'Brien PC, Weigand SD, Knopman DS, Boeve BF, Ivnik RJ, Smith GE, Cha RH,

- Tangalos EG, Petersen RC (2004) Comparison of different MRI brain atrophy rate measures with clinical disease progression in AD. *Neurology* **62**, 591-600.
- [43] Likeman M, Anderson VM, Stevens JM, Waldman AD, Godbolt AK, Frost C, Rossor MN, Fox NC (2005) Visual assessment of atrophy on magnetic resonance imaging in the diagnosis of pathologically confirmed young-onset dementias. *Arch Neurol* **62**, 1410-1415.
- [44] Davatzikos C, Resnick SM, Wu X, Parnpi P, Clark CM (2008) Individual patient diagnosis of AD and FTD via high-dimensional pattern classification of MRI. *Neuroimage* **41**, 1220-1227.
- [45] Fan Y, Resnick SM, Wu X, Davatzikos C (2008) Structural and functional biomarkers of prodromal Alzheimer's disease: a high-dimensional pattern classification study. *Neuroimage* **41**, 277-285.
- [46] Funke SA, Birkmann E, Willbold D (2009) Detection of Amyloid-beta aggregates in body fluids: a suitable method for early diagnosis of Alzheimer's disease? *Curr Alzheimer Res* **6**, 285-289.